B. C. Syamala RAO *
N. S. Lakshmana RAO **
AND
K. SEETHARAMIAH ***

CAVITATION EROSION ON ALUMINIUM IN A VENTURI SET-UP

Introduction

Although it had been noted for long, that the rate of material loss due to cavitation is not uniform with respect to time, some of its consequences have received attention only recently. Thiruvengadam and his co-workers [1] reported that characteristic erosion-time curves could be described in terms of four zones:

a) Incubation zone with no weight loss;

b) Accumulation zone with loss of rate increasing to a peak;

c) Attenuation zone with decreasing loss rate and finally:

d) Steady-state zone with constant loss rate (Fig. 1). They suggested that the final zone should be used for comparison or correlation purposes of different materials. But Plesset and Devine [2] disputed the sequential location of the attenuation zone and remarked that the maximum erosion continued for a certain period at a steady-state rate and then decreased (Fig. 2). The investigations of Hobbs [3] also showed trends similar to those of Figure 2. All these investigations [1, 2, 3] were conducted using magnetostriction oscillators. Working with a venturi type of set-up, Hammitt [4] found that there were numerous peaks and valleys in the erosion-time curve and it did not

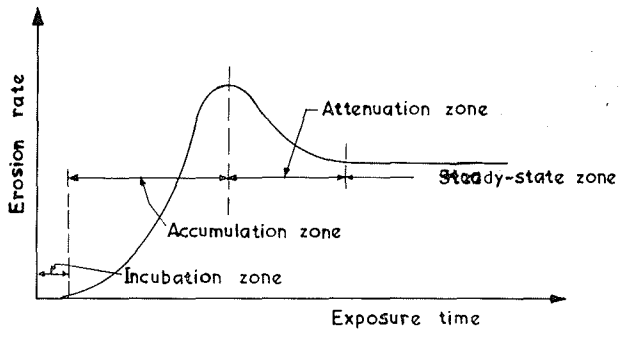

1/ Characteristic rate-time curve according to Thiruvengadam [1].
Courbe caractéristique du taux d'érosion en fonction du temps, d'après Thiruvengadam [1].

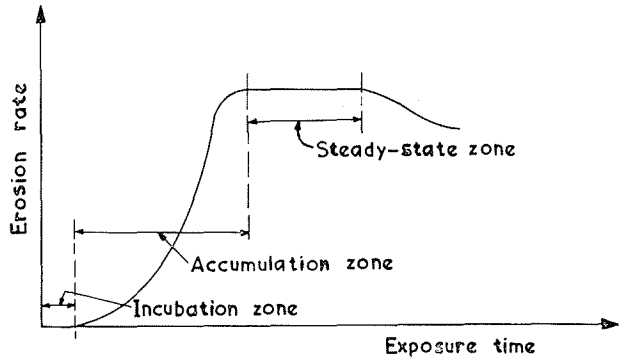

2/ Characteristic rate-time curve according to Plesset and Devine [2].
Courbe caractéristique du taux d'érosion en fonction du temps, d'après Plesset et Devine [2].

* Lecturer, Civil and Hydraulic Engineering Department, Indian Institute of Science, Bangalore, India.

** Associate Professor, Civil and Hydraulic Engineering Department, Indian Institute of Science, Bangalore, India.

*** Professor—in-charge, Civil and Hydraulic Engineering Department, Indian Institute of Science, Bangalore, India.

level off at any stage. Heymann [5], while presenting a critical review of the investigations on this subject proposed a statistical model for the prediction of some of the observed erosion-time curves.

It is known that the cavitation erosion rate is highly accelerated in a magnetostriction equipment compared to the same that occurs in most hydraulic systems. The investigations presented in this paper were conducted in a two-dimensional water-tunnel, causing cavitation behind a circular cylinder. The erosion was measured on aluminium whose mechanical properties are given in Table 1. These investigations reveal that on an average the ratetime curve can be divided into the three zones shown in Figure 2. In the final zone, the rate of erosion increased further instead of decreasing as in Figure 2. An interesting finding of this study is that there are numerous peaks and valleys in each characteristic zone and is not a simple smooth curve as observed in the accelerated tests.

It is generally agreed by all the investigators that the different characteristic zones of the rate-time curve are influenced by the changes in surface roughness caused by cavitation on the test specimen [6]. However, so far, no systematic measurements of the changes in surface roughness of the test specimen were measured. The present study includes such measurements at 20 minute intervals of test. The formation and growth of pits caused by cavitation and the resulting erosion were also studied macrographically at 5 × and a few macrographs are presented in the paper. Micrographs at 250 ×, of the individual cavitation pits with respect to the grain structure of aluminium are also presented. These investigations help in explaining the progress of cavitation erosion through the different characteristic zones as it occurs in most hydraulic systems.

The paper also presents an empirical equation for the prediction of the rate of cumulative erosion and cumulative erosion up-to a period seven times the incubation period.

Experimental equipment and procedure

Equipment.

The experiments were conducted in a two-dimensional water tunnel (Fig. 3). The tunnel consisted of a 6 in. dia pipe-line with a pressure regulating manifold, a by-pass needle valve, contraction cone, test-section and diffuser. The contraction cone was designed to transform the 6 in. dia circular cross section to a 4 in. × 1/2 in. rectangular section with a uniform change in pressure and velocity. The details of the test section with the position of the test specimens and the cavitating body are shown in Figure 4. Two test specimens were mounted on either wall with the cavitating body, 1/2 in. thick, 3/4 in. dia, extending fully over the width of the test section. The front side of the test section was provided with a transparent perspex cover.

Table 1

Mechanical Properties of Aluminium

Ultimate tensile strength.....	7.0 tons/in^2
Fatigue strength.	3.5 tons/in^2
Brinnell Hardness.	28.0
Strain Energy.	1,150.0 psi

Procedure.

Aluminium test specimens, 1/8 in. thick, were prepared to the desired size and their initial weight was determined. The specimens were fixed in the test section of the water tunnel and subjected to cavitation action for 20 min. The tests were conducted at a flow velocity of 90 fps., Reynolds number of 6.17×10^5 and an ambient pressure of 56.0 psi. At this velocity and other test conditions, the erosion caused on specimens in venturi is fairly severe and the velocity falls in the critical range in which the volume eroded increased rapidly with velocity to an average exponent of 15 [7]. The specimens were removed after 20 min. test and their weight determined. The procedure was repeated with the same pair of specimens for every 20 min. test up-to a cumulative time of 1 000 min. by which time the specimens were badly damaged and eroded. Before each weighing, the test specimens were washed in clean water, dried with a hair drier and cooled in a desiccator. To check the variation in weight loss with test time and to verify the difference in weight loss when the specimens were tested continuously and intermittently, different pairs of specimens were also tested for all the test periods up-to 440 min. at intervals of 10 min.

Analysis of the experimental data

Analysis of the weight loss measurements.

Figure 5 to 7 present the variations of the cumulative erosion in mg/m, rate of erosion in mg/min. and the rate of cumulative erosion in mg/hour. The rate of erosion in any interval is computed as the loss in weight of the specimens during that interval divided by the duration of the interval and is plotted at the end of that interval. The rate of cumulative erosion is computed as the cumulative erosion divided by the cumulative time. Figure 6 shows that on an average the erosion rate-time curve can be divided into the three zones proposed by Plesset and Devine [2], Figure 2. However, when the erosion process is not accelerated as in the case of magnetostriction oscillators, each characteristic zone consists of a number of peaks and valleys. Also, in the present study, the final zone exhibited erosion at a higher rate than the steady-state rate unlike the decreasing rate report-

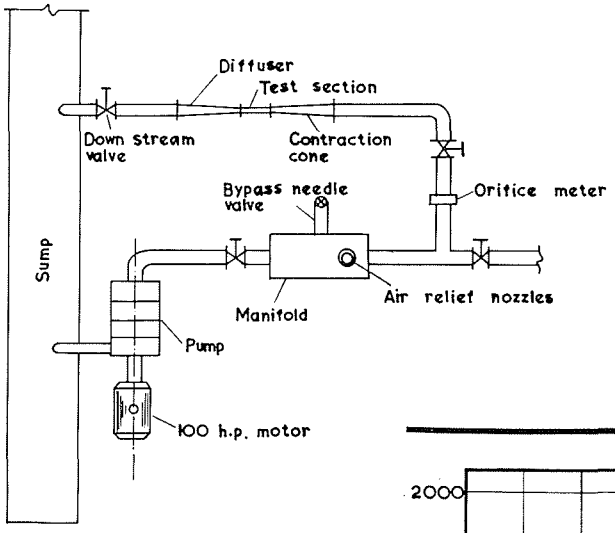

3/ Lay-out of the two-dimensional water tunnel.
Schéma du tunnel hydraulique à écoulement plan.

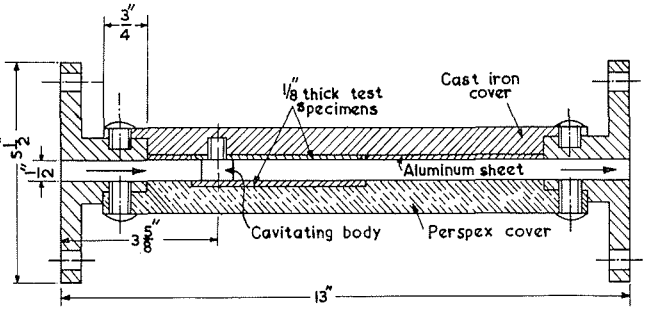

4/ Sectional plan of the water tunnel test section.
Coupe de la section d'essai du tunnel hydraulique.

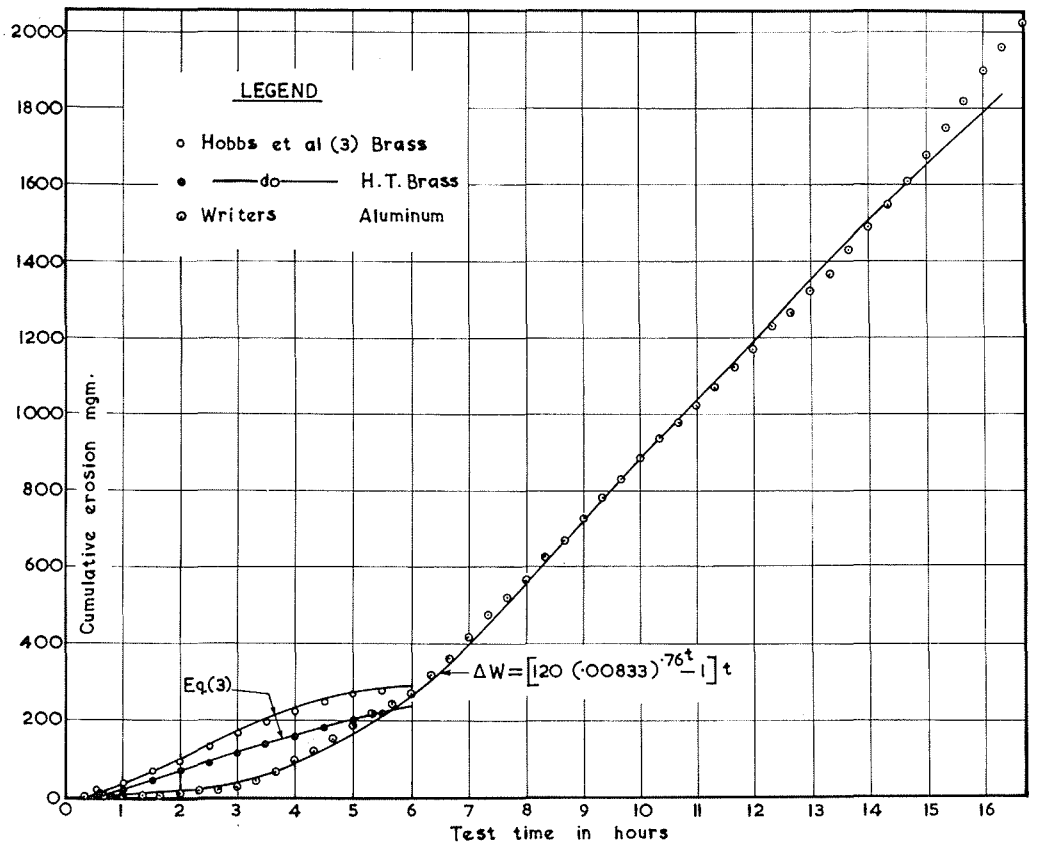

5/ Cumulative cavitation erosion-time curve.
Courbe cumulée de l'érosion de cavitation en fonction du temps.

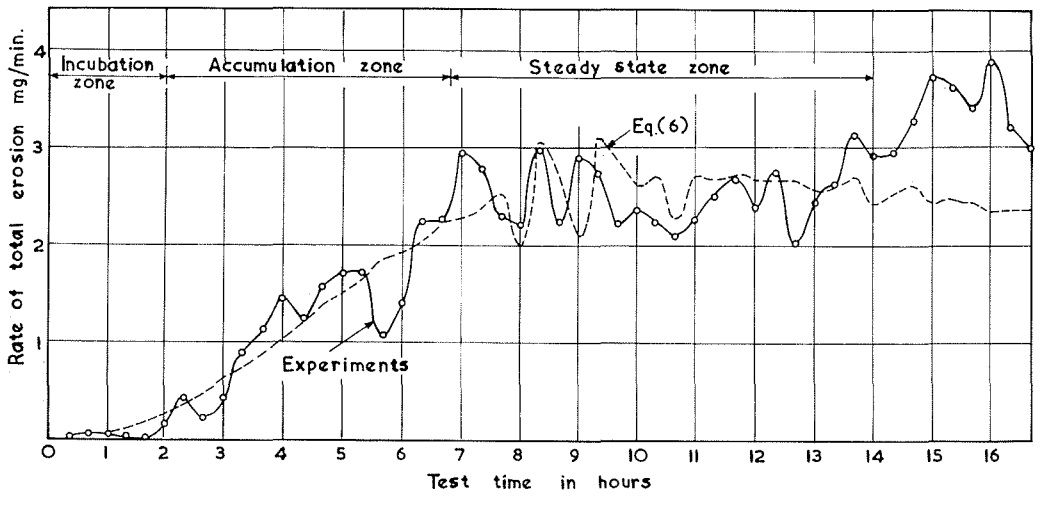

6/ Rate of cavitation erosion-time curve.
Courbe du taux d'érosion de cavitation en fonction du temps.

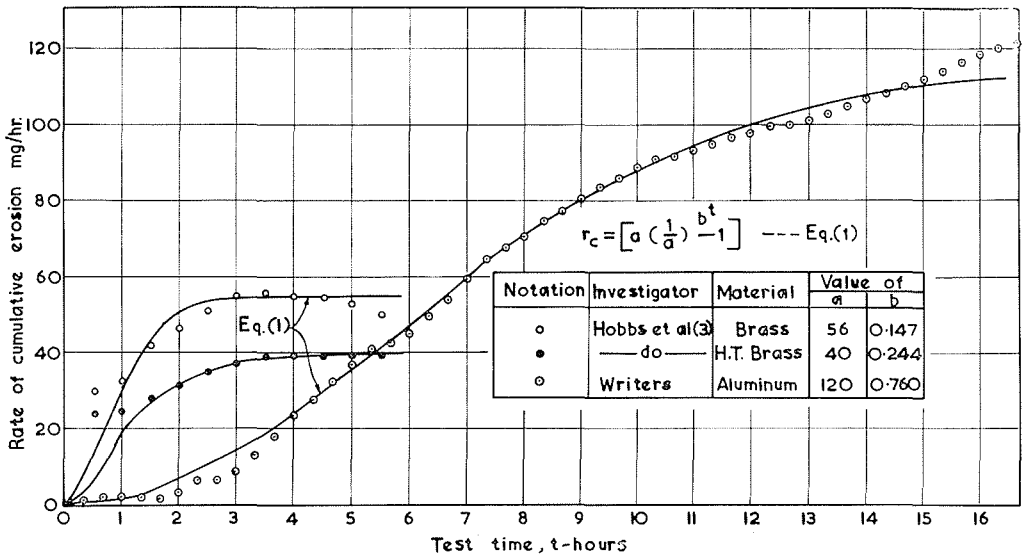

7/ Rate of cumulative cavitation erosion-time curve.
Courbe d'érosion de cavitation cumulée en fonction du temps.

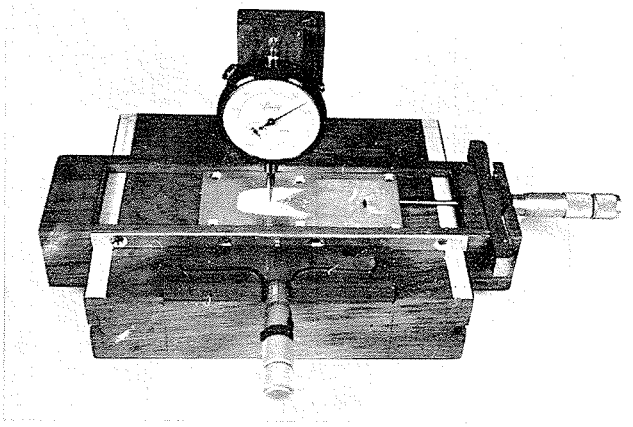

8/ Profilometer for measuring the surface roughness of the test specimens.
« Profilomètre » de mesure de la rugosité superficielle des échantillons d'essai.

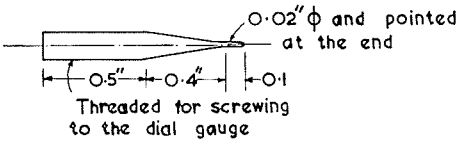

9/ Brass stylus used for the dial gage.
Style en laiton de la jauge à cadran.

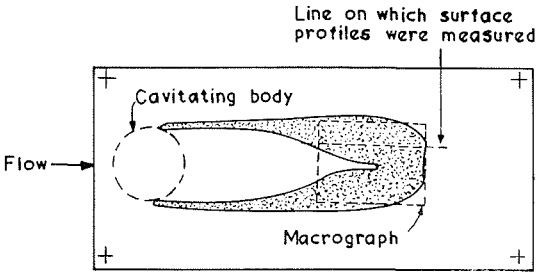

10/ Test specimen and cavitation erosion.
Echantillon d'essai et érosion de cavitation.

ed by other investigators (Fig. 2). This trend is believed to be the result of the loss in elastic properties of all the layers of the comparatively thin (1/8 in. thick) specimens exposed to erosion in the present study. Figure 7 indicates that the rate of cumulative erosion-time relationship is a smooth curve unlike that of rate of erosion-time.

Measurement of surface roughness.

Generally, all the investigators are in agreement that the different characteristic zones of the erosion rate-time curve are influenced by the changes in the hydrodynamic conditions caused by the variations in the surface roughness of the test specimens due to cavitation. However, so far no systematic measurements of the variations in surface roughness of the test specimens were made by any investigator, mostly because, the roughness caused by cavitation is too large to be measured on commercial roughness measuring equipment. Hence, in order to get detailed information on the variations in surface roughness caused by cavitation, a profilometer shown in Figure 8 was specially designed and fabricated by the writers. The profilometer consisted of two micrometers to give longitudinal and lateral movement to the test specimen to an accuracy of 0.001 in. and a dial gage to measure the surface profiles to an accuracy of 0.0001 in. The dimensions of the brass stylus used for the dial gage are shown in Figure 9. The profilometer is hand operated and each measurement is time consuming. The surface profiles were measured on one specimen at the end of every 20 min. cavitation test along a chosen line representing maximum damage characteristics shown in Figure 10.

Figure 11 presents some of the representative surface profiles of the test specimen at different test durations. It may be seen that in the first 60 min. there are hardly a few indentations and pits have just started forming. Towards the end of the incubation stage and immediately following that (100 min. to 160 min.) the pits grow in size and depth rapidly. As the test duration increases further (240 min. to 280 min.) a number of thin peaks and deep and wide valleys are formed. Also, some

of the peaks, A, B, C, D and E that appear at any interval vanish in the succeeding interval and these contribute to the loss in weight of the specimen. Figure 12 shows to an exaggerated scale a cross section of the aluminium test specimen subjected to damage at a test time of 400 min.

Macroscopic observations.

The formation and growth in size and number of pits caused by cavitation and their relative positions on the test specimen was studied macroscopically at 5×. Two such typical macrographs at test times of 170, and 200 min. are shown in Figures 13 and 14. After 30 min. test it was observed that the pits have just started forming at isolated locations. At 170 min., Figure 13, the pits are very well formed and there are a few over lappings of adjacent pits. As the test time increased (200 min. and above) the pits increased considerably in size and there are many overlappings of adjacent pits.

From the study of the variation in loss of weight and the variation in surface profiles of the test specimens and the macroscopic observations of the pitting it is possible to visualize the process of material erosion as the cavitation test duration increases. At the beginning of the test when the surface of the test specimen is smooth and flat it of-

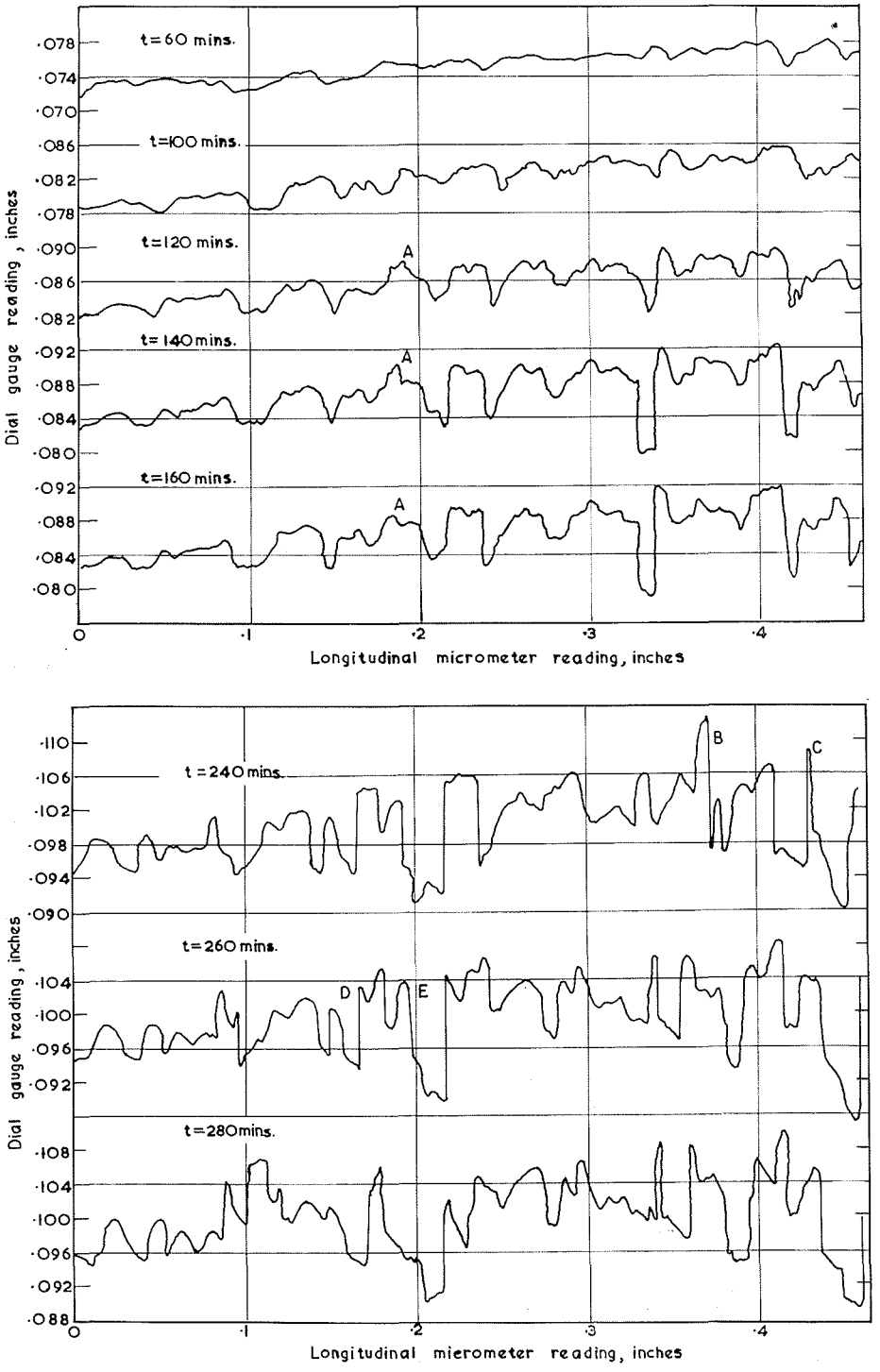

11/ Surface profiles of the test specimen.
Profils superficiels de l'échantillon d'essai.

fers an unfavourable surface to the pressure waves associated with the collapse of cavities. As the specimen surface is repeatedly attacked by the pressure waves it starts loosing its elastic properties and small indentations much similar to those formed by a hardness indentor are formed. However, at the very beginning of the test there is a small weight loss due to the erosion of some of the weak spots on the surface of the specimen. Thereafter, the weight loss is almost zero for a certain period and this is termed as the "incubation period". Towards the end of the incubation zone the specimen surface looses much of its elastic properties and plastic flow of the material sets in rapidly resulting in the formation of pits with peaks and valleys. At this stage the specimen offers a very favourable surface for erosion to occur and hence the rate of erosion increases to a peak value over a length of test period. This is the accumulation zone. After this, the formation of peaks and valleys and the erosion of the peaks proceeds simultaneously with the weight loss of the specimen exhibiting more or less a steady rate with test time. If the tests are accelerated or if the observation of weight loss in specimen made at larger intervals of time, all the three zones of the rate-time curve would appear as smooth curves observed by some investigators [2, 3]. On the contrary, if the tests are not accelerated and the observations made at close intervals of time, all the three zones of the rate-time curve, Figure 6, show a number of peaks and valleys indicating non-uniform erosion rate even in any characteristic zone.

Also, from a study of the surface profiles of the test specimen (Fig. 11), the material erosion in the present investigations can be said to be taking place in the following way: when peaks and valleys are formed on the specimen surface, the peaks are chipped off due to the shearing action of the radial outflow of the liquid from the adjacent pits. A similar observation was reported by Bowden and Brunton [8] also while investigating the erosion caused by the high speed impact of liquids.

Microscopic observations.

It is generally known that cavitation pitting is influenced by grain size [1, 4] of the specimen and the location of pits is affected by the grain boundaries [5]. The writers made microscopic observations at 100× and 250× of the locations of the pits with respect to the grain boundaries at different levels from the specimen surface. The specimens were polished and etched with concentrated Keller's etch for these observations. Figures 15 and 16 show some typical cavitation pits observed at the same magnification at a depth of 6.2 mm from the original surface. The pit boundaries are very irregular and are located randomly with respect to the grain structure of the specimen.

Prediction of cavitation erosion

One of the important aspects of the investigations of the nature presented in this paper is to know whether the cavitation erosion of a given material under given hydrodynamic conditions can be predicted. The writers have attempted to define the rate-time curve, Figure 6, through a series of sine functions and the rate of cumulative erosion-time curve, Figure 7, through an empirical equation. The latter attempt was more successful than the former and the shape of the rate of cumulative erosion-time curve was found to conform to that of the Gompertz curve, generally used in statistics. The curve is of the form:

$$y = a\left(\frac{1}{a}\right)^{b^x} - 1 \qquad (1)$$

in which, a and b are coefficients; and x and y are the abscissa and ordinate respectively.

The coefficients a and b were determined by trial and error from the experimental data of Figure 7 and Equation (1) conforming to the présent study was found to be:

$$r_c = 120\left(\frac{1}{120}\right)^{0.76^t} - 1 \qquad (2)$$

in which, r_c = rate of cumulative erosion in mg/hour; and t = test time in hours. Equation (2) was found to be reasonably accurate up-to a period of 6-7 times the incubation period. The cumulative erosion (Δw/mg) with test time is obtained from Equation (1) as:

$$\Delta w = r_c t = \left[a\left(\frac{1}{a}\right)^{b^t} - 1\right] t \qquad (3)$$

For aluminium used in the present studies Equation (3) can be written as:

$$\Delta w = \left[120\left(\frac{1}{120}\right)^{0.76^t} - 1\right] t \qquad (4)$$

The rate of erosion during any test interval is found to be:

$$r = \frac{\Delta w_2 - \Delta w_1}{t_2 - t_1} \qquad (5)$$

in which subscripts 1 and 2 refer to quantities at the two instants of time. Substituting for Δw from Equation (4) in Equation (5) yields:

$$r = \frac{[120\,(1/120)^{0.76^{t_2}} - 1]\,t_2 - [120\,(1/120)^{0.76^{t_1}} - 1]\,t_1}{t_2 - t_1} \qquad (6)$$

Equations (4) and (6) are shown in Figures 5 and 6 respectively. It may be seen that the cumulative erosion is predicted fairly well by Equation (4) up-to a period of 6-7 times the incubation period.

Figure 7 also presents the variation of the rate of cumulative erosion with test time for the experimental data of Hobbs et al. [3] for brass and high tensile brass. It may be seen that Equation (1) fits the data with reasonable accuracy. The values of the coefficients a and b in Equation (1) for these two materials are given in the figure. Figure 5 presents the variation of cumulative erosion with time for these two materials also. A similar extensive analysis by the writers of the experimental data of

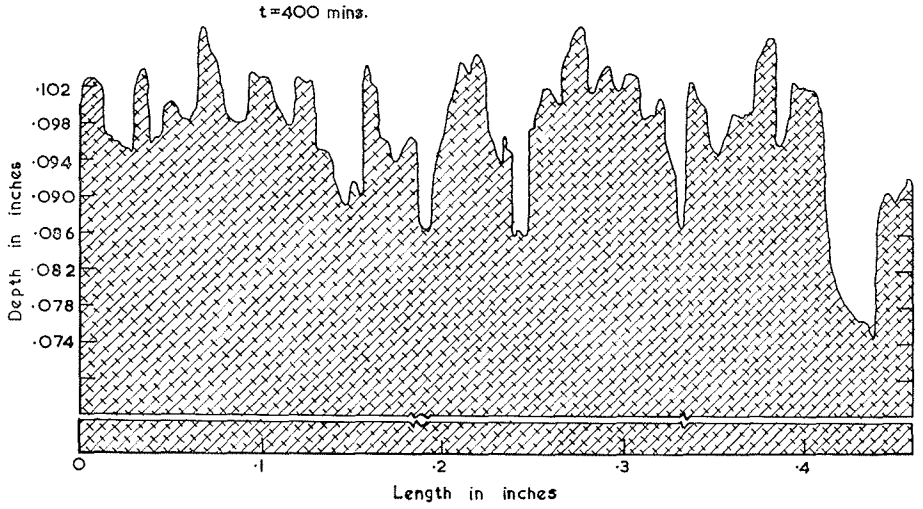

12/ Cross-section of the aluminium test specimen at 400 mins.
Section transversale de l'échantillon d'essai en aluminium au bout de 400 mn.

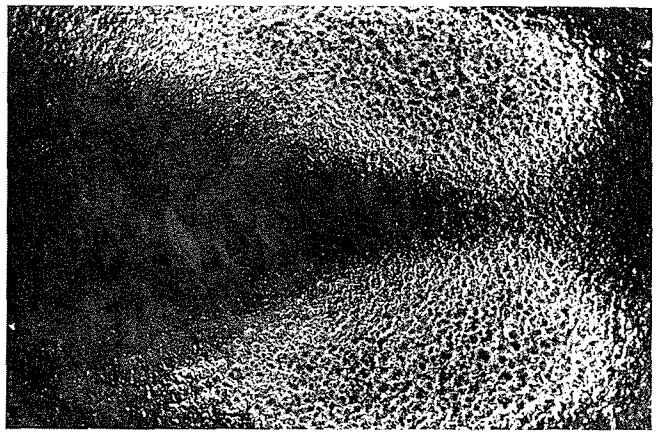

13/ Macrograph of cavitation pitting at test time of 170 mins.
Macrographie des cratères de cavitation au bout de 170 mn.

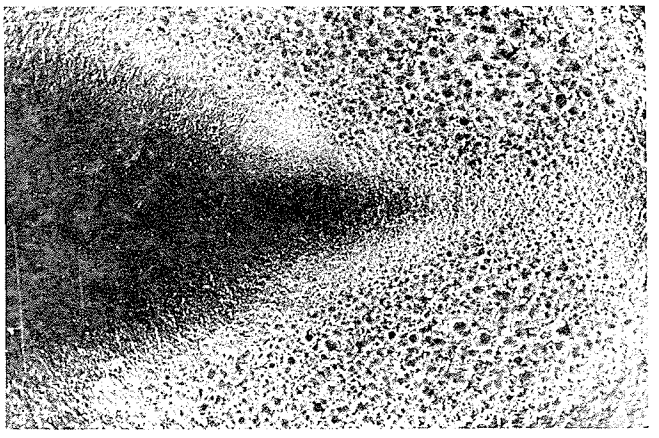

14/ Macrograph of cavitation pitting at test time of 200 mins.
Macrographie des cratères de cavitation au bout de 200 mn.

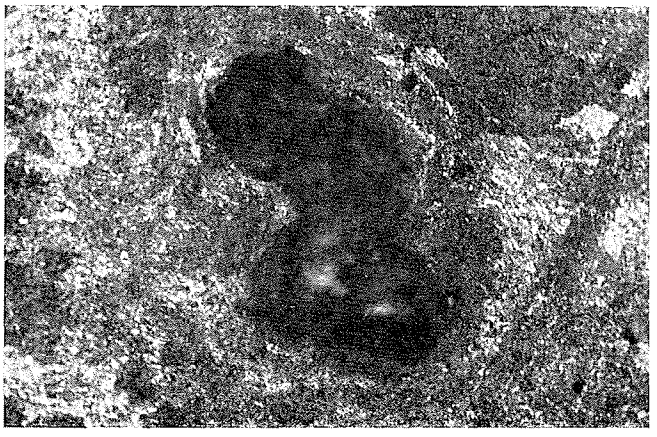

15/ Micrograph of individual cavitation pit (250 ×, etched).
Micrographie d'un cratère de cavitation (attaqué à l'acide, grossi 250 fois).

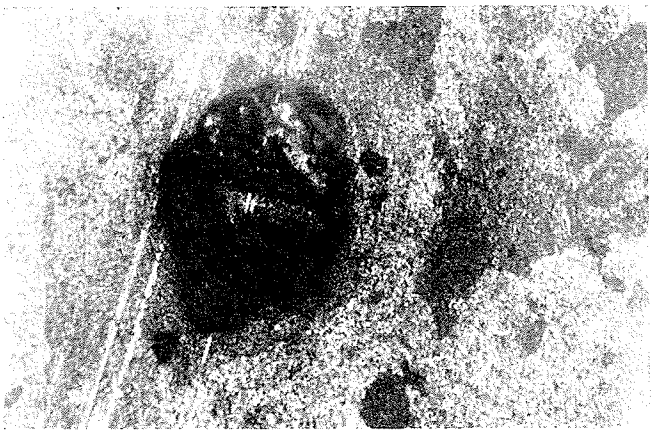

16/ Micrograph of individual cavitation pit (250 ×, etched).
Micrographie d'un cratère de cavitation (attaqué à l'acide, grossi 250 fois).

other investigators shows that Equation (1) defines the rate of cumulative erosion with time with dependable accuracy up-to the end of the steady-state zone. More experimental data to determine the dependence of the coefficients a and b in Equation (1) on the mechanical properties of the materials and the hydrodynamic conditions of the flow will be useful to the profession.

Conclusions

1. The cavitation erosion rate-test time curve of aluminium tested in a venturi set-up exhibited three characteristic zones, namely, incubation, accumulation and steady-state zones. In each zone peaks and valleys showing non-uniform rate of erosion were found unlike the smooth curves in the accelerated tests.

2. The measurements of the test specimen surface profiles and macroscopic observations of cavitation pitting revealed that during the incubation period the specimen surface exposed to cavitation was damaged to a shape favourable for erosion. In the accumulation zone the specimen lost its elastic properties and plastic flow occurred rapidly with erosion rate increasing to a peak. In the steady-state zone plastic flow of the material around pits and the erosion occurred simultaneously at more or less a constant rate.

3. Microscopic observation of individual cavitation pits with respect to the grain boudaries of the specimen showed that they were randomly located and the boundaries of the pits were very irregular.

4. The variation of cumulative erosion with test time observed in the present investigations could be defined by an equation of the type:

$$\Delta w = \left[120\left(\frac{1}{120}\right)^{0.76^t} - 1\right] t \qquad (7)$$

Equation (7) can be used for predicting cavitation erosion under similar hydrodynamic conditions upto a period of 6-7 times the incubation period.

Bibliography

[1] Eisenberg (P.), Preiser (H.S.) and Thiruvengadam (A.). — On the Mechanism of Cavitation Damage and Methods of Protection. Presented at the Annual Meeting of the Society of Naval Architects and Marine Engineers (November, 1965).

[2] Plesset (M.S.) and Devine (R.E.). — Effect of Exposure Time on Cavitation Damage. *Journal of Basic Engineering*, Trans. ASME, Vol. 88 D, No. 4 (December 1966), pp. 691-705.

[3] Hobbs (J.M.), Laird (A.) (Miss) and Brunton (W.C.). — Laboratory Evaluation of the Vibratory Cavitation Erosion Test. National Engineering Laboratory, East Kilbride, Glasgow, Report No. 271 (January 1967).

[4] Hammitt (F.G.), Robinson (M.J.), Siebert (C.A.) and Aydinmakine (F.A.). — Cavitation Damage correlations for various Fluid-Material Combinations. Report No. 03424-14-J, Dept. of Nuclear Engg. Univ. of Michigan (October 1964).

[5] Heymann (F.J.). — On the Time Dependence of the Rate of Erosion due to Impingement or Cavitation. Erosion by Cavitation or impingement, ASTM STP 408, (1967), pp. 70-109.

[6] Seetharamiah (K.), Lakshmana Rao (N.S.) and Syamala Rao (B.C.). — Discussion of "Glen Canyon Dam Diversion Tunnel Outlets", by W.E. Wagner, *Journal of the Hydraulics Division*, ASCE, Vol. 94, No. HY 4, (July 1968), pp. 1156-1158.

[7] Syamala Rao (B.C.) Lakshmana Rao (N.S.) and Seetharamiah (K.). — "The effect of Flow Velocity on Cavitation Erosion". Presented at the 38th C.B.I.P. Annual Meeting held at Bangalore (June 1968).

[8] Bowden (F.P.) and Brunton (J.H.). — The Deformation of Solids by Liquid Impact at Supersonic Speeds. *Proceedings Royal Society of London*, A, Vol. 263 (1961), pp. 433-450.